Journal of Structural Geology, Vol. 7, No. 5, pp. 503 to 511, 1985
Printed in Great Britain

0191-8141/85 $03.00 + 0.00

Deformation of granitic rocks across the brittle–ductile transition

CAROL SIMPSON

Department of Geological Sciences, Virginia Polytechnic Institute and State University, Blacksburg, VA 24061, U.S.A.

(*Received* 4 *July* 1984; *accepted in revised form* 17 *January* 1985)

Abstract—A microstructural analysis has been carried out on mylonites and mylonitic gneisses of the Eastern Peninsular Ranges Mylonite Zone, which were formed over a range of metamorphic conditions from lower greenschist to amphibolite facies. Composite planar fabrics in the form of C and S planes are found at all metamorphic grades. Fractured feldspars, kinked biotites and ductile deformation of quartz characterize the lower greenschist facies mylonites. At mid-upper greenschist grade orthoclase grains show dynamic recrystallization textures whereas plagioclase exhibits low temperature plasticity with only minor recovery. Biotite ribbons form by progressive rotation and coalescence of kink band segments to produce chevron fold patterns. At epidote–amphibolite grade and above, recovery processes and annealing recrystallization predominate in all minerals. Residual orthoclase porphyroclasts show strain-related myrmekite formation along those sides of the grains that face the instantaneous shortening direction. Myrmekite formation due to replacement reactions cannot explain this geometry. It is proposed that the myrmekites formed due to a combination of exsolution, replacement and strain-enhanced diffusion.

INTRODUCTION

DEFORMATION of quartzo-feldspathic rocks at the brittle–ductile transition in deep-seated fault zones commonly produces mylonites in which quartz and mica deform in a ductile manner whereas feldspars show brittle deformation features (e.g. Debat *et al.* 1978, Berthé *et al.* 1979, Tullis 1979, Watts & Williams 1979, White *et al.* 1980, Tullis *et al.* 1982, White & White 1983). The transition from brittle to brittle–ductile bulk rock behaviour in quartz-rich rocks is thought to be determined mainly by the response of quartz to changes in applied stress and temperature (e.g. Sibson 1983). Mylonites formed under greenschist facies conditions exhibit a reduction in overall grain size from that of the undeformed rock (Tullis *et al.* 1982) but often contain residual feldspar porphyroclasts that show little or no reduction in grain size. In contrast, mylonitic gneisses, which are the deeper-level equivalents of such mylonites (Watterson 1979), often show very little overall reduction in grain size in comparison to their undeformed protolith. Mylonitic gneisses generally contain evidence for complete recovery of all constituent minerals (Theodore 1966, 1970, Voll 1976, Simpson 1982) and seldom contain true porphyroclasts, although the augen in some augen gneisses may have originated as porphyroclasts (e.g. Vidal *et al.* 1980, Simpson 1981).

The transition from fully ductile to completely brittle behaviour of quartzo-feldspathic rocks occurs over so wide a range of physical conditions (i.e. temperature, confining pressure, fluid pressure, strain rate, etc.) that it is almost impossible to find a single naturally occurring shear zone/fault in which the entire spectrum is encompassed. Therefore, most studies of naturally deformed rocks have been, of necessity, confined to relatively narrow ranges of deformation conditions.

This paper contains the results of a detailed microstructural analysis of a suite of mylonites that grade into mylonitic gneisses across the Eastern Peninsular Ranges Mylonite Zone in Southern California (Fig. 1). Evidence exists for the progressively more ductile behaviour of feldspars (plagioclase and orthoclase) with increase in metamorphic grade. Strain-related myrmekitic intergrowths and ribbon biotites are well preserved in these rocks, and possible models for their formation are presented.

GEOLOGICAL SETTING

The Eastern Peninsular Ranges Mylonite Zone (EPRMZ) is a major west-directed thrust that extends southward from Palm Springs, California to the tip of Baja California (Sharp 1966, 1967, 1979, Simpson 1984a) (Fig. 1). Most of the rocks affected by the EPRMZ are mid-Cretaceous granodiorites, tonalites, quartz diorites and quartz monzonites of the Peninsular Ranges batholith, with minor local involvement of Mesozoic and Palaeozoic metasedimentary rocks (Sharp 1966, 1979, Theodore 1970, Todd & Shaw 1979, Anderson 1983, Simpson 1984a). Fission-track and K–Ar studies have yielded an upper age limit of 61–63 Ma for the deformation in the Santa Rosa Mylonite Zone (SRMZ) section of the EPRMZ (Dokka & Frost 1978, Wallace & English 1982, Dokka 1984).

Post-Pliocene offset along the still active right-lateral San Jacinto fault zone has divided the EPRMZ into three major fault blocks (Dibblee 1954, Sharp 1967, 1979, Bartholomew 1970) (Fig. 1). From north to south these are (i) the Santa Rosa mylonite zone between Palm Springs and the San Jacinto/Clark fault, (ii) the Coyote Mountain mylonite zone between the San

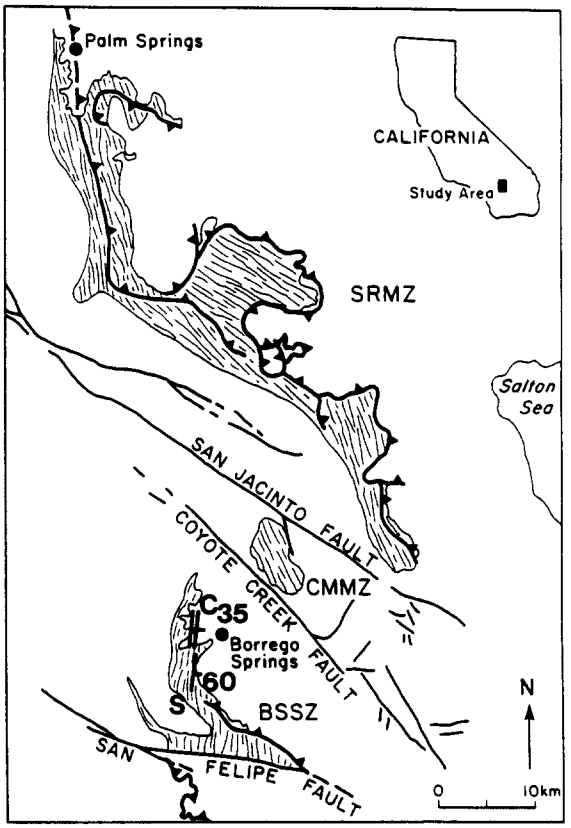

Fig. 1. Simplified geological sketch map of the studied portion of the Eastern Peninsular Ranges Mylonite Zone (EPRMZ), southern California (modified after Sharp 1979). SRMZ, Santa Rosa Mylonite Zone; CMMZ, Coyote Mountain Mylonite Zone; BSSZ, Borrego Springs Shear Zone. Light lines indicate general distribution and foliation trends of the EPRMZ. S, schistosity; C, cisaillement (shear) planes. Medium lines represent faults of the San Jacinto system. Heavy lines with teeth indicate Tertiary thrust and/or detachment faults.

Jacinto/Clark and Coyote Creek faults and (iii) the Borrego Springs shear zone between the Coyote Creek and San Felipe faults (Fig. 1). Differential uplift of the three fault blocks has resulted in present-day exposure of different structural levels of the EPRMZ (Sharp 1979). Sillimanite-bearing mylonites that indicate upper amphibolite facies deformation conditions occur in the Coyote Mountain block (Theodore 1966, 1970, Anderson 1983). Most of the mylonites of the Santa Rosa block formed under lower to middle amphibolite facies conditions (Anderson 1983, Simpson 1984b). In contrast, the Borrego Springs section contains mylonites that formed predominantly under upper greenschist facies conditions (Simpson 1984a), although conditions vary locally from lowest greenschist to lowest amphibolite facies. These three fault blocks thus allow a documentation of the changes in microstructures with progressive increase in temperature and pressure of deformation. Mesoscopic features associated with the thrust zone vary from well-foliated mylonites and ultramylonites (Theodore 1970, Anderson 1983), to S-C mylonites (where C stands for 'cisaillement' or localized high-strain shear plane, and S stands for the finite strain-related schistosity; for detailed discussion of S-C mylonites see Berthé *et al.* 1979, Simpson & Schmid 1983, Simpson 1984a, Lister & Snoke 1984, Snoke *et al.* 1985).

In order to facilitate a direct comparison between samples, the metasedimentary units were excluded from the present study. Only those mylonites derived from the quartz-rich igneous rocks are described here. Oriented thin sections were cut perpendicular to foliation and parallel to the mineral elongation lineation in the rock. Mineral composition analyses were carried out using an ARL electron microprobe.

MICROSTRUCTURAL VARIATIONS WITH INCREASING METAMORPHIC GRADE

A detailed petrological and petrographic description of the rocks of the Peninsular Ranges Batholith is contained in Todd & Shaw (1979). Anderson (1983) has carried out an extensive petrological study of both the undeformed rocks and mylonites of the EPRMZ. All of the undeformed granitic rocks retain their original igneous textures, although close to the margins of the EPRMZ most of the rocks have undergone some strain. Minor shear zones of a few metres or less in width occur sporadically near to the margin of the EPRMZ. Quartz grains in the slightly strained rocks outside the shear zones show undulose extinction, with subgrain formation and recrystallization around their margins giving rise to a core-and-mantle structure (White 1976). Rarely, feldspar crystals contain microfractures, and biotite crystals are kinked.

Deformation at lower greenschist grade

Under lower greenschist facies conditions (zo–chl–bi–qtz–or–an), all quartz grains deformed predominantly by dislocation creep to produce a well developed ribbon structure (Fig. 2a) with deformation bands at a high angle to the ribbon boundaries. Minor recovery resulted in subgrains and recrystallized new grains (average diameter 5 μm) in irregular patches and along some of the ribbon boundaries, which correspond to Type 1 polycrystalline quartz ribbons of Boullier & Bouchez (1978). Biotite contains simple, open kink bands (Fig. 2b), and all of the feldspar grains (An_{23}–An_{36} and orthoclase) have undergone grain size reduction by microcracking and microfaulting (Fig. 2a). Where these microfaults are at a high angle to the mylonitic foliation, the sense of movement on them is antithetic to the overall shear sense in the rock; where at a low angle to the mylonitic foliation, they show a sympathetic sense of shear (cf. Etchecopar 1974, 1977). Progressive rotation of the microfault-blocks resulted in a greater physical separation of feldspar fragments along the foliation with increase in bulk strain. In tonalites and diorites, hornblende underwent grain size reduction by cataclasis and shows minor replacement by chlorite.

Deformation at mid-upper greenschist grade

Under middle to upper greenschist facies conditions, quartz retains a residual ribbon texture but has under-

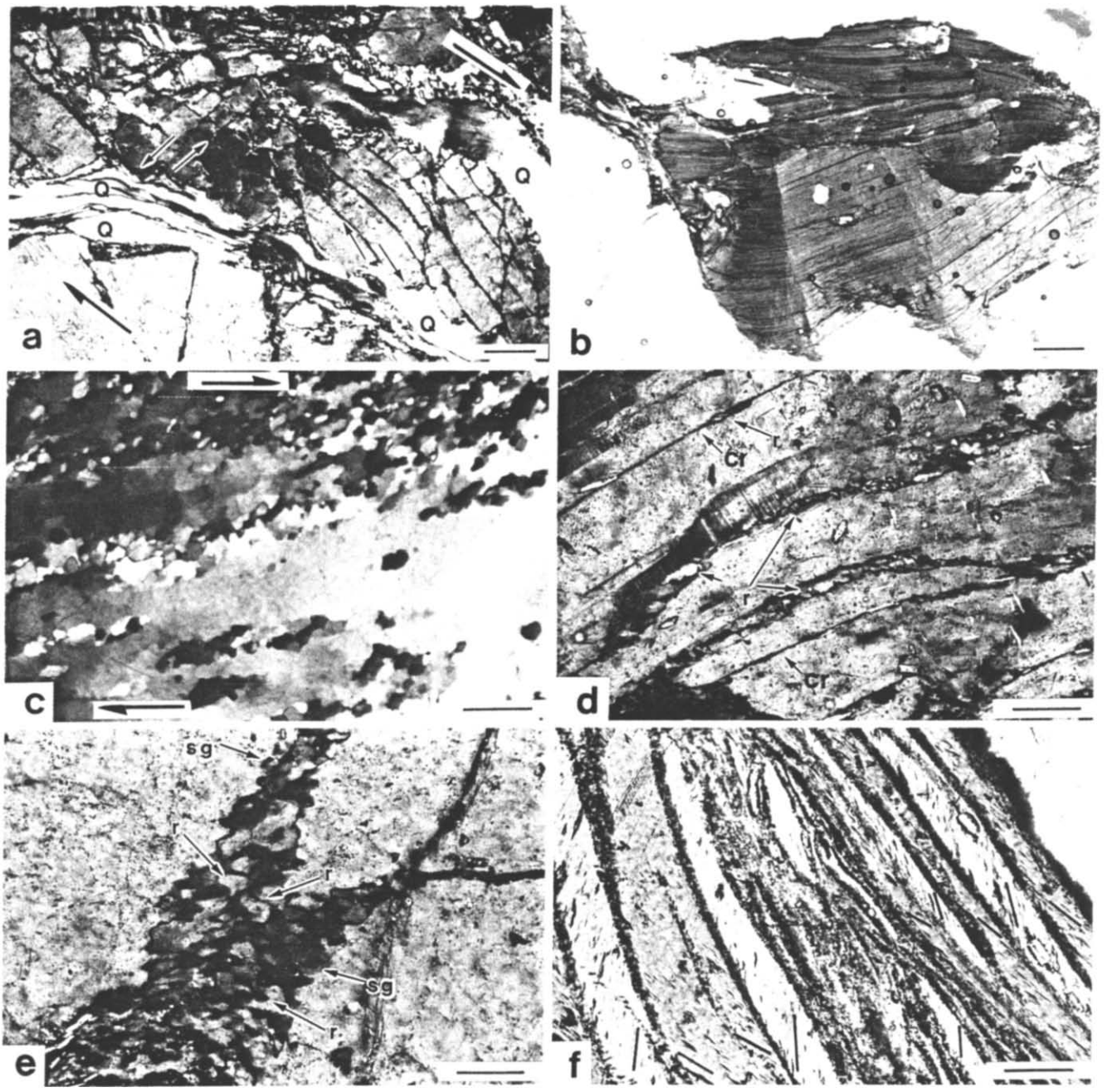

Fig. 2. Mylonite microstructures typical of lower greenschist facies (a, b) and middle greenschist facies (c, d, e, f) deformation conditions. (a) Multiple fracturing of orthoclase grains in a ductile quartz-ribbon matrix (Q). Small arrows indicate relative movement along the microfaults; large arrows indicate overall dextral shear sense for the mylonite. (b) Biotite showing simple, open kink bands. (c) Polygonal elongate recrystallized quartz grains within quartz ribbons of middle greenschist facies mylonites of the SRMZ. Arrows indicate overall dextral shear sense for the mylonite. (d) Plagioclase (An_{35}) with small recrystallized grains (r) along curviplanar microcracks (cr). (e) Orthoclase showing subgrains (sg) and recrystallized new grains (r) along relatively planar zones in the host crystal. (f) Ribbon biotite structure with ilmenite and finely recrystallized biotite along ribbon boundaries. (001) cleavage planes (accentuated by heavy lines) are symmetrically distributed about the ribbon boundaries. All photomicrographs taken with crossed nicols except for (b) and (f). Scale bars for (a) and (b) are 250 μm, for (c), (d), (e) and (f) 100 μm.

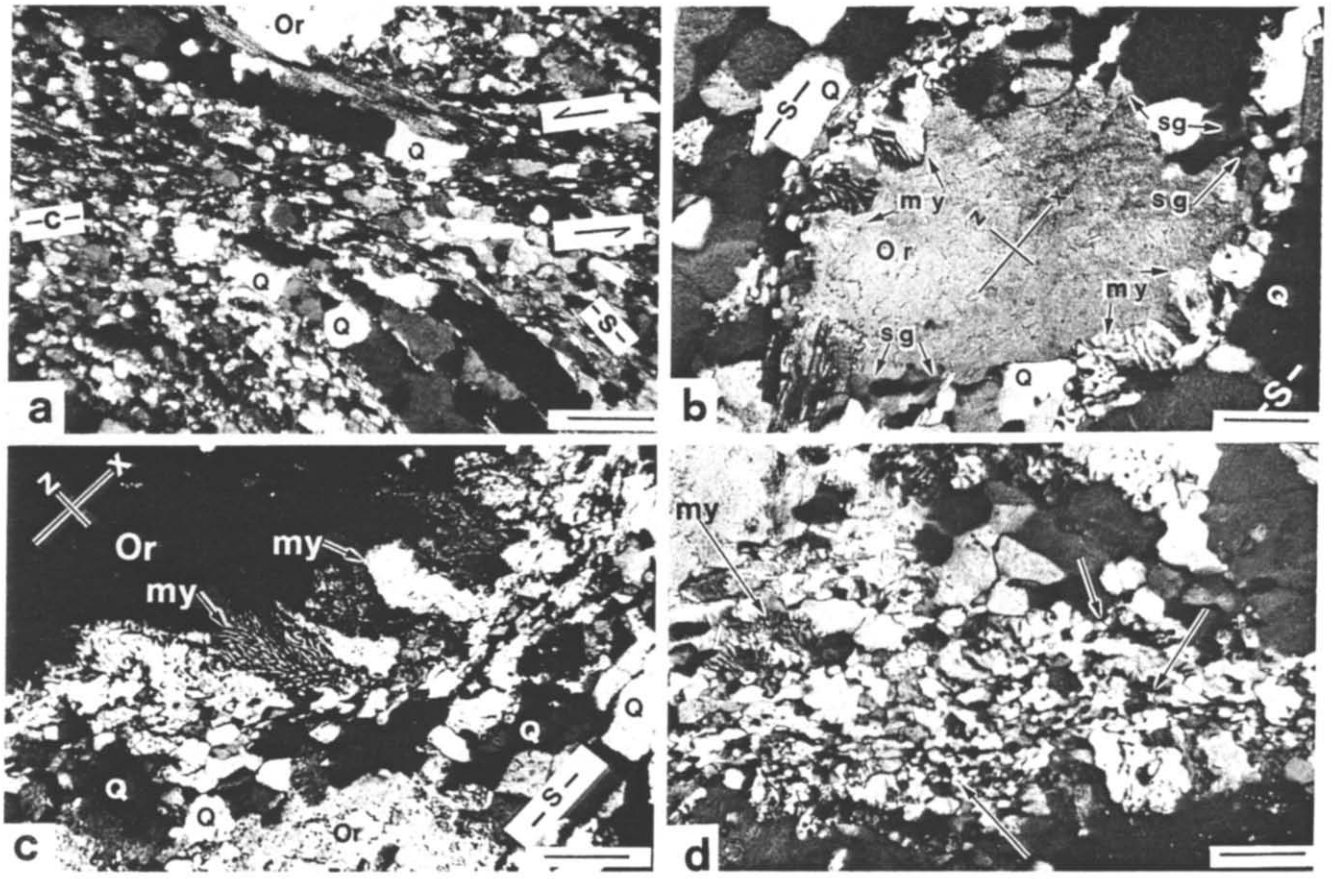

Fig. 3. Mylonitic granodiorite from epidote–amphibolite zone of the SRMZ. (a) Composite planar fabric comprising S planes and a C (cisaillement, shear) plane. All minerals show complete recovery and a progressive decrease in grain size as the S planes curve asymptotically into the left-lateral C plane. Q, quartz; Or, orthoclase. (b) An orthoclase porphyroclast (Or) preserved between S planes. Angular, bulbous myrmekitic intergrowths (my) occur on the two sides of the porphyroclast that face the finite shortening direction, Z, for the S planes. Subgrains and recrystallized new grains of orthoclase (sg) occur on the two sides of the porphyroclast that face X. (c) Comma-shaped morphology of myrmekitic intergrowths at edge of orthoclase porphyroclast (Or). Sense of shear known from independent evidence to be left-lateral. (d) Fine-grained quartz/albite/orthoclase zone from within a C plane. Vermicular texture is present throughout (small arrows). Distinct myrmekitic texture is preserved in patches (arrowed my). All photomicrographs taken with crossed nicols. Scale bar for (a) is 250 μm, for (b), (c) and (d), 100 μm.

gone considerable recovery (Fig. 2c) to produce elongate, recrystallized new grains 15 μm in diameter (Type 2 ribbons of Boullier & Bouchez 1978). The planes of flattening of the new elongate grains tend to face the direction of instantaneous shortening. Plagioclase (An_{35}) shows evidence for low temperature plasticity in the formation of kink bands (Fig. 2d), and minor recrystallization along curvi-planar microcracks can be observed (Fig. 2d). Electron microprobe analyses of the host and recrystallized grains show a slight reduction in An content with recrystallization (from An_{35} to An_{27}). Orthoclase grains contain narrow planar zones of finely recrystallized material of average grain size 15 μm (Fig. 2e). The presence of 5–15 μm diameter subgrains (i.e. less than 10° optical misorientation) along the host orthoclase grain margins suggests that the recrystallized grains initially formed by progressive misorientation of subgrains (Poirier & Nicolas 1975) and not by simple annealing of cataclastically deformed feldspar fragments. In some zones, orthoclase grains are almost entirely recrystallized to a fine-grained mosaic of average grain size 2–5 μm and only small, isolated porphyroclasts of the host orthoclase remain. Electron microprobe analyses of host and recrystallized orthoclase grains show no detectable differences in composition.

Deformation of biotite grains under middle greenschist facies conditions occurs predominantly by kink-band formation. A distinctive biotite ribbon structure is observed in some samples (Fig. 2f), in which biotite (001) planes in adjacent ribbons are symmetrically inclined at about 30° to planar ribbon boundaries. No evidence was found for jagged kink-band boundaries such as have been described by Etheridge & Hobbs (1979) and Wilson & Bell (1979). A progressive reorientation of material within kink bands, together with recrystallization of very fine-grained new biotite and ilmenite grains along the kink-band boundaries could account for the formation of the biotite ribbons. This mechanism is analogous to that of chevron fold formation as an end-product of kinking in a multilayered sequence (Paterson & Weiss 1966, Starkey 1968, Weiss 1969, Etheridge *et al.* 1973, Bell 1979, Wilson & Bell 1979).

Deformation at epidote–amphibolite and higher grades

At epidote–amphibolite facies conditions and above, well preserved quartz ribbons (Type 3 of Boullier & Bouchez 1978) are ubiquitous in quartz rich EPRMZ mylonites, and help to define a gneissosity. The average grain size of quartz within the ribbons is in the range 100–300 μm. In areas of well developed S-C mylonites (Lister & Snoke 1984), a reduction in quartz grain size to about 30 μm occurs as the S planes curve into the C, or shear, planes (Fig. 3a). The presence of high angle grain boundaries and strain free grains within the quartz ribbons suggests that the quartz is almost completely recovered and recrystallized. Biotite and muscovite grains are completely recrystallized in these rocks and are aligned such that their (001) planes are subparallel to the margins of the quartz ribbons. Plagioclase grains are also recrystallized to a polygonal mosaic with an average grain size of 50 μm. However, in the S-C mylonites well preserved orthoclase porphyroclasts occur between the quartz ribbons that define the S planes: it is these porphyroclasts that contain evidence for strain-related myrmekite formation.

Strain-related myrmekites

Figure 3(b) shows a typical orthoclase porphyroclast ($Ab_{9.0}An_{0.5}Or_{90.5}$) from the amphibolite facies zone of the EPRMZ in a region of uniformly developed S-C mylonites. The angle between S and C planes is approximately 43°. On the two sides facing the maximum finite elongation direction (X) for the S foliation, there are 50 μm diameter subgrains and recrystallized new grains of orthoclase ($Ab_{7.0}An_{0}Or_{93.0}$). However, the two sides of the porphyroclast that face the maximum finite shortening direction (Z) for the S foliation have well developed myrmekitic quartz/oligoclase (An_{28}) intergrowths. In the majority of cases, the edges of myrmekitic intergrowths that face into the host crystal are angular (Fig. 3b) suggesting that some recovery has taken place. Occasionally, the intergrowths show a smooth and rounded bulbous morphology. Rarely, comma-shapes are seen (Fig. 3c) where the 'tails' of the myrmekitic intergrowths are deflected into the matrix that surrounds the host porphyroclast, with the sense of deflection being the same as the sense of shear across the mylonite zone. All of these relationships among myrmekitic intergrowths and host grains are illustrated schematically in Fig. 4.

Within the C planes, the mylonitic foliation only occasionally contains residual elongate orthoclase grains. Irregular zones of finer-grained (10 μm) admixtures of quartz/oligoclase/orthoclase are common (Fig. 3d). A vermicular texture can be seen throughout and preservation of distinct myrmekitic texture is seen in some areas (MY on Fig. 3d). Identification of the constituent minerals is almost impossible using optical microscopy but a series of electron microprobe traverses across several such fine-grained zones showed a random arrangement of individual orthoclase, quartz and oligoclase grains. Although a small proportion (*c.* 1%) of muscovite is found in the fine-grained regions, there is no obvious direct association of the muscovites and the myrmekitic textures.

DISCUSSION

Several features of the mylonites in the EPRMZ differ from previously published descriptions of mylonitic granitic rocks, even though the overall microstructures are familiar. In the discussion that follows, the behaviour of quartz, biotite and feldspar with changing metamorphic grade are treated separately.

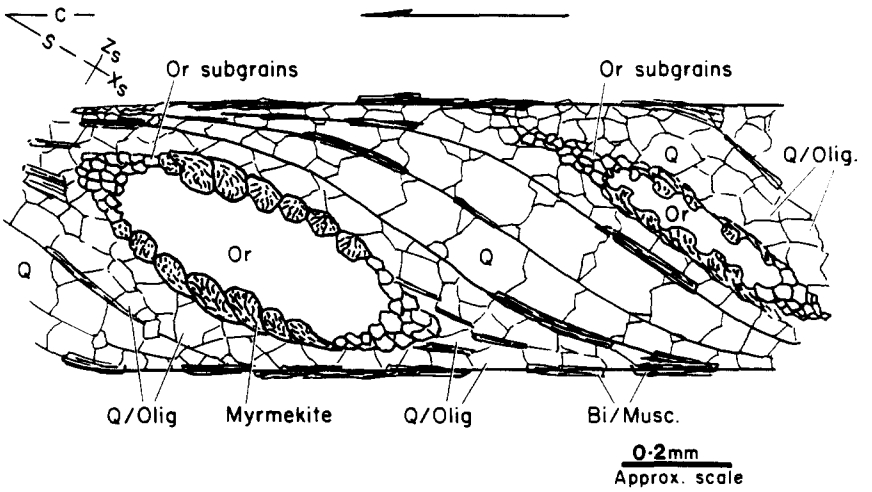

Fig. 4. Schematic diagram to illustrate the geometrical relationships among C and S planes, orthoclase porphyroclasts (Or), myrmekite zones, and orthoclase subgrains/recrystallized new grains. Z_s and X_s represent the finite strain axes for the S foliation only and do not represent the bulk finite strain axes for the rock.

Quartz

The degree of recovery of quartz in ribbons, and the size of recrystallized quartz grains, both increase with increasing metamorphic grade in the EPRMZ mylonites. Increased recovery is to be expected at higher temperatures since recovery involves the thermally activated climb of dislocations. However, according to Nicolas & Poirier (1976) and Tullis (1979), the dynamically recrystallized grain size should be relatively independent of temperature increase regardless of whether grain-boundary migration or subgrain rotation mechanisms were operative. The observed increase in recrystallized grain size with increase in temperature may reflect either (1) a decrease in the differential stress required to deform the rock (Twiss 1977, Mercier *et al.* 1977), or (2) a predomination of annealing recrystallization over dynamic recrystallization at the higher grades. Pinning of quartz grain boundaries by recrystallized biotite and feldspar grains may help to preserve the smooth outlines of the ribbon texture even above amphibolite grade (Simpson 1982).

Biotite

In the greenschist facies mylonites, biotite deforms by slip on (001) to produce primary kink bands (Etheridge *et al.* 1973). At epidote–amphibolite grade the observed increase in angle of bending, ω, of (001) across kink band boundaries is consistent with the experimental results of Etheridge *et al.* (1973) and Etheridge & Hobbs (1974). These authors show that coalescence of primary kink bands can form secondary kinks or chevron structures. However, the ribbon biotites of the SRMZ differ from the experimentally formed chevron structures by the presence of fine-grained recrystallized biotite and exsolved ilmenite along kink-band boundaries, suggesting that dynamic recrystallization accompanied the kinking (cf. Bell 1979, Wilson & Bell 1979). This process would result in a progressive reduction in grain size as well as a physical reorientation of the biotite (001) planes. At amphibolite facies and above, all biotites are completely recrystallized with their (001) planes subparallel to the foliation.

Plagioclase

Plagioclase in the EPRMZ mylonites undergoes a change in deformation mechanism from cataclasis in lower greenschist facies rocks, to low temperature plasticity (kink-band formation) in upper greenschist facies rocks. The localization of recrystallization along curviplanar fracture surfaces suggests that zones of high strain and/or already reduced grain size were a necessary prerequisite for recrystallization under these metamorphic conditions. Complete recrystallization to a polygonal mosaic at epidote–amphibolite grades and above supports the findings of Voll (1976), Hanmer (1982), and Tullis (1983) that plagioclase may undergo steady-state dislocation-creep processes at temperatures in excess of 450–500°C.

Orthoclase

Orthoclase in the EPRMZ mylonites undergoes brittle failure at lower greenschist grade. However, the presence of subgrains and zones of fine grained recrystallized orthoclase in middle to upper greenschist facies rocks, suggests that dislocation creep and dynamic recrystallization processes were operative (Simpson 1984b). No evidence for myrmekite formation was found in any of the low grade mylonites, but the ubiquitous presence of myrmekite in epidote–amphibolite grade mylonites, warrants a separate discussion.

Strain-related myrmekite formation

The presence of quartz–oligoclase myrmekitic intergrowths along the two sides of orthoclase grains facing

the finite shortening direction for the S planes, as well as within the finer grained C planes, is something of an enigma. Similar phenomena have been found in sheared adamellite of the Lepontine Alps (Simpson 1981), in mylonites of the Santa Catalina Complex in southern Arizona (Simpson, unpublished data) and have been illustrated (but not discussed) in a deformed microcline grain by Debat *et al.* (1978 fig. 1b). The two main hypotheses for myrmekite formation are (i) replacement reactions (Becke 1908) and (ii) solid-state diffusion and exsolution (Schwantke 1909) (see Phillips 1974, for discussion of these and other models for myrmekite genesis). A modification of the Becke (1908) replacement model is considered by Phillips (1980) to be the most applicable to myrmekites in deformed granitoids. According to the Becke model, Na and Ca are introduced, and K removed, along grain boundaries such that

$$KAlSi_3O_8 + Na^+ \rightarrow NaAlSi_3O_8 + K^+ \qquad (1)$$

and

$$2KAlSi_3O_8 + Ca^{2+} \rightarrow CaAl_2Si_2O_8 + 4SiO_2 + 2K^+ \qquad (2)$$

with the silica precipitating as vermicular quartz. A sodic plagioclase results from the mixing of albite and anorthite components (Becke 1908, Phillips 1980). According to Phillips (1980), with the introduction of water to the system, alkali feldspar might be converted to myrmekite and muscovite according to the reaction

$$\underset{\substack{\text{alkali}\\\text{feldspar}}}{\begin{pmatrix}3KAlSi_3O_8\\NaAlSi_3O_8\end{pmatrix}} + \underset{\substack{\text{calcic}\\\text{plagioclase}}}{\begin{pmatrix}CaAl_2Si_2O_8\\NaAlSi_3O_8\end{pmatrix}} + H_2O \rightarrow + \text{ water} \rightarrow \underbrace{\underset{\substack{\text{more sodic}\\\text{plagioclase}}}{\begin{pmatrix}CaAl_2Si_2O_8\\2NaAlSi_3O_8\end{pmatrix}} + 6SiO_2 + \text{ quartz}}_{\text{myrmekite}} + K_2O \qquad (3)$$

$$+ KAl_2(Al,Si_3)O_{10}(OH)_2 + \text{ muscovite}$$

For any of reactions (1)–(3) to proceed, removal of K_2O from the immediate system is required. The presence of water would not only favour growth of muscovite but would also facilitate the removal of any excess K_2O from the rock. Anderson (1983) has convincingly demonstrated that a large volume of predominantly H_2O fluid did pass through the EPRMZ mylonites during deformation. Thus, the Becke (1908) and Phillips (1980) replacement reactions could cause the myrmekite formation, but they cannot account for the strain-related configuration.

The stress field around an orthoclase grain is likely to be highly complex during progressive deformation. However, if the C planes are taken to be subparallel to the overall shear-zone boundary (Berthé *et al.* 1979, Lister & Snoke 1984), then the observed 43° angle between C and S planes suggests that instantaneous and finite shortening directions for the S planes are roughly parallel to one another. Under non-hydrostatic stress, dry rock at high temperatures may undergo diffusional creep, such that vacancies diffuse towards the instantaneous shortening direction, and interstitial or 'extra' atoms diffuse towards the extension direction (Nicolas & Poirier 1976, Tullis 1979). This deformation mechanism is slow and diffusional distances must be short (i.e. small grain size) for any significant strain to be accomplished. However, the addition of small amounts of water to the rock may speed up grain boundary diffusion significantly.

The Schwantke (1909) solid-state diffusion model for myrmekite formation requires that Na and Ca diffuse through an orthoclase grain to the site where myrmekite will form. A redistribution of Si and Al then occurs within the host grain/myrmekite interface (Phillips 1974, 1980). The following model for the strain-related configuration of the EPRMZ myrmekitic intergrowths combines this diffusion–exsolution model with the mechanism of diffusional creep.

In non-hydrostatically stressed orthoclase grains, cationic vacancies will be more mobile than anionic vacancies (Nicolas & Poirier 1976) and will tend to diffuse more rapidly towards the side of the grain that faces the instantaneous shortening direction. This diffusive flux will set up a charge imbalance unless cations also diffuse, in the same direction at a similar rate, to neutralize the charge. The ionic radius of Na^+ is considerably less than that of K^+ and, therefore, Na^+ could diffuse more quickly through the grain. White (1975) has demonstrated that for oligoclase, the effect of strain is to increase the diffusion rates of ionic species by at least a factor of ten. However, calcium cations, despite their small ionic radii, diffuse extremely slowly through feldspars (Paul H. Ribbe, personal communication) and are not thought to play a major role in this model. Thus, a concentration of sodium would tend to occur on the side of the grain facing the shortening direction, and myrmekite formation according to the Schwantke model could then occur in this position. Plagioclase grains in the vicinity could supply any additional calcium needed at the myrmekite site. In addition, the migration of sodium to the grain boundaries would allow the Becke (1908) replacement reactions to occur.

As summarized by Phillips (1980), the morphology of the myrmekitic intergrowths may play a role in deciding whether the Becke model or the Schwantke model best fits any given myrmekite association. A bulbous, invasive appearance, with quartz vermicules that project almost to the myrmekite/orthoclase interface, is usually interpreted to indicate the replacement reaction model of Becke (1908), or some combination of exsolution and replacement (Phillips 1980). If exsolution alone were to occur, Phillips (1980) has suggested that the boundaries of the myrmekitic intergrowths should be planar or gently curved. Some of the myrmekitic intergrowths of the EPRMZ rocks do have a bulbous and invasive appearance, but the majority have planar boundaries (Fig. 3b) and therefore cannot be attributed to the

replacement model alone: they are more likely due to a combination of both the diffusional creep–exsolution and the replacement models.

Deformation conditions in the EPRMZ

On the basis of an ultramylonite 'xenolith' within a less deformed tonalitic mylonite of the BSSZ section of the EPRMZ, Anderson (1983) has suggested that the EPRMZ was active prior to and during emplacement of the Peninsular Ranges batholith. Although the writer cannot refute Anderson's evidence, all of the microstructural features in the BSSZ are consistent with the rocks having been cooled to, or even below, lower greenschist conditions prior to their mylonitization. The presence of recrystallized planar fractures in the middle to upper greenschist facies mylonites of the SRMZ suggests that these rocks were also initially deformed at temperatures below the 500°C suggested by Anderson (1983). On the other hand, the complete absence of brittle deformation features in the epidote–amphibolite and higher grade mylonites of the SRMZ and CMMZ blocks is in agreement with temperatures in the range 580–600°C prior to and during mylonitization (Theodore 1970, Anderson 1983). This would be consistent with mylonite formation at greater depths within the EPRMZ thrust system.

CONCLUSIONS

Lower greenschist facies granitic mylonites of the EPRMZ show the typical brittle–ductile microstructural assemblage of ductilely deformed quartz, kinked biotite and fractured feldspars. The transition to textures indicative of completely ductile bulk rock behaviour occurs within the middle to upper greenschist facies range, as the feldspars begin to undergo ductile deformation by low temperature plasticity and dislocation creep. At epidote–amphibolite facies and above, the mylonites of the EPRMZ show no evidence for brittle deformation in any of the constituent minerals. The recrystallized grain size of quartz increases with metamorphic grade and is always greater than that of the associated feldspars. Myrmekite formation in these higher grade mylonites is geometrically related to the finite strain axes and a diffusional creep–exsolution model is proposed to explain this configuration.

Acknowledgements—Support for this work was provided by NSF grants EAR-812 1438 and EAR-830 5846. P. H. Ribbe kindly read the manuscript and provided helpful comments. Helpful discussions with F. D. Bloss, L. Dell'Angelo, G. V. Gibbs, J. Tullis and R. A. Yund are gratefully acknowledged. The manuscript was greatly improved by the comments of an anonymous referee. However, the author takes full responsibility for the interpretations contained herein. I thank T. N. Solberg for assistance with electron microprobe analyses, M. B. Rafalowski for assistance in the field, E. Frost for invaluable logistical support, L. S. Sharp for photographic assistance, S. Chiang for drafting the figures, and H. Evans-Wardell and P. Sullivan for secretarial assistance.

REFERENCES

Anderson, J. R. 1983. Petrology of a portion of the Eastern Peninsular Ranges mylonite zone, southern California. *Contr. Miner. Petrol.* **84**, 253–271.

Bartholomew, M. J. 1970. San Jacinto Fault Zone in the northern Imperial Valley, California. *Bull. geol. Soc. Am.* **81**, 3161–3166.

Becke, F. 1908. Ueber Myrmekite. *Schweiz. miner. petrog. Mitt.* **27**, 377–390.

Bell, T. H. 1979. The deformation and recrystallization of biotite in the Woodroffe Thrust mylonite zone. *Tectonophysics* **58**, 139–158.

Berthé, D., Choukroune, P. & Jegouzo, P. 1979. Orthogneiss, mylonite and non-coaxial deformation of granites: the example of the South Armorican Shear Zone. *J. Struct. Geol.* **1**, 31–42.

Boullier, A-M. & Bouchez, J-L. 1978. Le quartz en rubans dans les mylonites. *Bull. Soc. geol. Fr.* **7**, 253–262.

Debat, P., Soula, J. C., Kubin, L. & Vidal, J. L. 1978. Optical studies of natural deformation microstructures in feldspars (gneisses and pegmatites from Occitanie, southern France). *Lithos* **11**, 133–146.

Dibblee, T. W., Jr. 1954. Geology of the Imperial Valley region, California. *Bull. California Div. Mines and geol.* **170** (2), 21–28.

Dokka, R. K. 1984. Fission-track geochronological evidence for late Cretaceous mylonitization and early Paleocene uplift of the northeastern Peninsular Ranges, California. *Geophys. Res. Lett.* **11**, 46–49.

Dokka, R. K. & Frost, E. G. 1978. Fission track ages from the Santa Rosa mylonite and its protolith and their relation to the cooling history of the southern California batholith. *Geol. Soc. Am. Abstr. Progr.* **10**, 103.

Etchecopar, A. 1974. Simulation par ordinateur de la deformation progressive d'un aggregat polycristallin. Etude du developpement de structures orientées par ecrasement et cisaillement. Unpublished thesis, Université de Nantes, France.

Etchecopar, A. 1977. A plane kinematic model of progressive deformation in a polycrystalline aggregate. *Tectonophysics* **39**, 121–139.

Etheridge, M. A. & Hobbs, B. E. 1974. Chemical and deformational controls on recrystallization of mica. *Contr. Miner. Petrol.* **43**, 111–124.

Etheridge, M. A., Hobbs, B. E. and Paterson, M. S. 1973. Experimental deformation of single crystals of biotite. *Contr. Miner. Petrol.* **38**, 21–36.

Hanmer, S. K. 1982. Microstructure and geochemistry of plagioclase and microcline in naturally deformed granite. *J. Struct. Geol.* **4**, 197–214.

Lister, G. S. & Snoke, A. W. 1984. S-C mylonites. *J. Struct. Geol.* **6**, 617–638.

Mercier, J.-C., Anderson, D. A. & Carter, N. L. 1977. Stress in the lithosphere: inferences from steady state flow of rocks. *Pure appl. Geophys.* **115**, 199–226.

Nicolas, A. & Poirier, J.-P. 1976. *Crystalline Plasticity and Solid State Flow in Metamorphic Rocks*. Wiley, New York.

Paterson, M. S. & Weiss, L. E. 1966. Experimental deformation and folding in phyllite. *Bull. geol. Soc. Am.* **77**, 343–374.

Phillips, E. R. 1974. Myrmekite—one hundred years later. *Lithos* **7**, 181–194.

Phillips, E. R. 1980. On polygenetic myrmekite. *Geol. Mag.* **17**, 29–36.

Poirier, J.-P. & Nicolas, A. 1975. Deformation—induced recrystallization due to progressive misorientation of subgrains with special reference to mantle peridotites. *J. Geol.* **83**, 707–720.

Schwantke, A. 1909. Die Beimischung von Ca im Kalifeldspat und die Myrmekitbildung. *Zentralblatt Miner. geol. Palaeont.*, 311–316.

Sharp, R. V. 1966. Ancient mylonite zone and fault displacements in the Peninsular Ranges of southern California. *Spec. Pap. geol. Soc. Am.* **101**, 333.

Sharp, R. V. 1967. San Jacinto fault zone in the Peninsular Ranges of southern California. *Bull. geol. Soc. Am.* **78**, 705–730.

Sharp, R. V. 1979. Some characteristics of the eastern Peninsular Ranges mylonite zone. In: *Proceedings, Conference VIII—Analysis of Actual Faults in Bedrock*, U.S. Geol. Survey Open File Rpt. 79-1239, 258–267.

Sibson, R. H. 1983. Continental fault structure and the shallow earthquake source. *J. geol. Soc. Lond.* **140**, 741–767.

Simpson, C. 1981. Ductile shear zones: a mechanism of rock deformation in the orthogneisses of the Maggia Nappe, Ticino, Switzerland. Unpublished Ph.D. thesis, ETH Zurich.

Simpson, C. 1982. Strain and shape fabric variations associated with ductile shear zones. *J. Struct. Geol.* **5**, 61–72.

Simpson, C. 1984a. Borrego Springs–Santa Rosa mylonite zone: a late

Cretaceous west-directed thrust in southern California. *Geology* **12**, 8–11.

Simpson, C. 1984b. Ductile deformation of feldspars in mylonitic granodiorite, Santa Rosa Mylonite Zone, California. *Geol. Soc. Am. Abst. with Progr.* **16**, 63.

Simpson, C. & Schmid, S. M. 1983. An evaluation of criteria to deduce the sense of movement in sheared rocks. *Bull. geol. Soc. Am.* **94**, 1281–1288.

Snoke, A. W., Tullis, J. A. & Todd, V. R. in press. Atlas of mylonites and fault-related rocks. Springer-Verlag, Heidelberg.

Starkey, J. 1968. The geometry of kink bands in crystals—a simple model. *Contr. Miner. Petrol.* **19**, 133–141.

Theodore, T. J. 1966. The fabric of a high-grade mylonite zone in Southern California (abstract). *EOS (Am. Geophys. Un. Trans.)* **47**, 491–492.

Theodore, T. J. 1970. Petrogenesis of mylonites of high metamorphic grade in the Peninsular Ranges of Southern California. *Bull. geol. Soc. Am.* **81**, 435–450.

Todd, V. R. & Shaw, S. E. 1979. Structural, metamorphic and intrusive framework of the Peninsular Ranges batholith in southern San Diego County, California. In: *Mesozoic Crystalline Rocks* (edited by Abbott, P. L. & Todd, V. R.) Geol. Soc. Am. Annual Meeting Field Trip Guidebook, San Diego State University, San Diego, 177–231.

Tullis, J. A. 1979. High temperature deformation of rocks and minerals. *Rev. Geophys. Space Phys.* **17**, 1137–1154.

Tullis, J. A. 1983. Deformation of feldspars. In: *Feldspar Mineralogy* (edited by Ribbe, P. H.). Miner. Soc. Am., short course notes, Vol. 2 (2nd Edn), 297–323.

Tullis, J. A., Snoke, A. W. & Todd, V. R. 1982. Penrose Conference report: significance and petrogenesis of mylonitic rocks. *Geology* **10**, 227–230.

Twiss, R. J. 1977. Theory and applicability of a recrystallized grain size paleopiezometer. *Pure appl. Geophys.* **115**, 227–244.

Vidal, J.-L., Kubin, L., Debat, P. & Soula, J.-C. 1980. Deformation and dynamic recrystallization of K feldspar augen in orthogneiss from Montagne Noire, Occitania, southern France. *Lithos* **13**, 247–255.

Voll, G. 1976. Recrystallization of quartz, biotite, and feldspars from Erstfeld to the Leventina Nappe, Swiss Alps, and its geological significance. *Schweiz. miner. petrog. Mitt.* **56**, 641–647.

Wallace, R. D. & English, D. J. 1982. Evaluation of possible detachment faulting west of the San Andreas, southern Santa Rosa Mountains, California. In: *Mesozoic–Cenozoic Tectonic Evolution of the Colorado River Region, California, Arizona, and Nevada* (edited by Frost, E. G. & Martin, D. L.), Cordilleran Publishers, San Diego, 503–509.

Watterson, J. 1979. Strain and strain rate gradients at the ductile levels of fault displacements. In: *Proceedings, Conference VIII—Analysis of Actual Faults in Bedrock*, U.S. Geol. Survey Open-File Rpt. 79-1239, 235–257.

Watts, M. J. & Williams, G. D. 1979. Fault rocks as indicators of progressive shear deformation in the Guingamp region of Brittany. *J. Struct. Geol.* **1**, 323–332.

Weiss, L. E. 1969. Flexural slip of foliated model materials. In: *Proceedings, Conference on Research in Tectonics (Kinkbands and Brittle Deformation)*, Geol. Surv. Can. Paper, 68–52.

White, S. H. 1975. Tectonic deformation and recrystallization of plagioclase. *Contr. Miner. Petrol.* **50**, 287–304.

White, S. H. 1976. The effects of strain on the microstructures, fabrics and deformation mechanisms in quartzites. *Phil. Trans. R. Soc.* **A283**, 69–86.

White, S. H., Burrows, S. E., Carreras, J., Shaw, N. D. & Humphreys, F. J. 1980. On mylonites in ductile shear zones. *J. Struct. Geol.* **2**, 175–187.

White, J. C. & White, S. H. 1983. Semi-brittle deformation within the Alpine fault zone, New Zealand. *J. Struct. Geol.* **5**, 579–590.

Wilson, C. J. L. & Bell, I. A. 1979. Deformation of biotite and muscovite: optical microstructure. *Tectonophysics* **58**, 179–200.